Thermoset Architecture Fusion Enabled by Catalyst-Free C=C/C=N Metathesis Chemistry

Jie Zheng,[a,*] Wendy Rusli,[a] Karen Yuanting Tang,[b] Wei Peng Goh,[b] Ning Ding, [b] Sheau Wei Chien,[b] Nikos Hadjichristidis,[c,*] Zibiao Li [a,b,d,*]

[a] Institute of Sustainability for Chemicals, Energy and Environment (ISCE^2), Agency for Science, Technology and Research (A*STAR), 1 Pesek Road, Jurong Island, Singapore 627833, Republic of Singapore.

[b] Institute of Materials Research and Engineering, Agency for Science, Technology, and Research (A*STAR), 2 Fusionopolis Way, Innovis #08-03, Singapore 138634, Republic of Singapore.

[c] Polymer Synthesis Laboratory, Chemistry Program, Physical Sciences and Engineering Division, KAUST Catalysis Center, King Abdullah University of Science and Technology (KAUST), Thuwal 23955, Saudi Arabia.

[d] Department of Materials Science and Engineering, National University of Singapore, 9 Engineering Drive 1, Singapore 117576, Republic of Singapore.

Correspondence to: zheng_jie@isce2.a-star.edu.sg; nikolaos.hadjichristidis@kaust.edu.sa; lizb@imre.a-star.edu.sg.

Abstract:

Thermosets with permanent crosslinked structures provide excellent durability but pose significant challenges for reprocessing and recycling, raising engineering and environmental concerns as their usage expands. The advent of covalent adaptable networks (CANs) with dynamic covalent linkages has improved thermoset recyclability and enabled the fusion of identical polymer networks (A-A type fusion). However, fusing different thermosets (A-B type fusion) remains challenging due to their distinct dynamic behaviors and variable activation energies for bond exchange. This study introduces catalyst-free solid-state C=C/C=N metathesis chemistry to achieve A-B type fusion between two distinct thermosets. Furthermore, by simply adjusting the mixing ratio of the parent thermosets, the thermal behavior, mechanical properties, activation energy (E_a), and topology freezing transition temperature (T_v) of the fused networks can be precisely tailored. This approach offers enhanced control over thermal and mechanical characteristics, rendering them suitable for diverse high-performance applications. Our findings represent a significant step forward in developing recyclable thermosets with improved engineering performance, contributing to advancing a more sustainable circular economy.

1. Introduction

Thermosets are three-dimensional (3D) polymer networks with covalent crosslinks formed during the curing process, rendering the entire structure a single molecular unit.[1–5] Their highly crosslinked structure, impart excellent mechanical strength, as well as thermal and chemical stability, making them the material of choice for various modern plastic products. Annually, over 65 million tons of thermosets are produced, representing approximately 18% of all polymeric materials manufactured globally.[6] However, the permanent crosslinked structure that provides these benefits also makes thermosets challenging to reprocess and recycle, significantly contributing to plastic waste accumulation. Addressing this issue by developing thermosets with enhanced reprocessibility and recyclability has become a critical and urgent challenge.

Covalent adaptable networks (CANs) represent a new class of materials that bridge the gap between thermosets and thermoplastics, attracting significant attention in recent years.[4,7–10] By incorporating dynamic covalent bonds into polymer networks, CANs enable covalently crosslinked polymers to undergo stimuli-responsive reprocessing similar to thermoplastics while maintaining the high mechanical strength, dimensional stability, and chemical/solvent resistance characteristic of thermosets under service conditions. Among CANs, "vitrimers" stand out as a particularly remarkable subset due to their use of an associative bond exchange mechanism.[11] This mechanism preserves a consistent crosslinking density during processing, ensuring superior dimensional stability and extended material performance. Numerous associative exchange reactions, such as transesterification,[12–16] transamination,[17–19] transthioetherification, [20–22] and silyl ether exchange, [23–25] have been explored for the development of vitrimers, demonstrating their versatility and potential in advanced material applications. However, the efficient occurrence of these

exchange reactions often requires the presence of active nucleophilic groups, such as hydroxyl, amino, or thiol groups, which can lead to undesired side reactions and deterioration in material performance.[26,27] To address these challenges, dynamic covalent metathesis chemistry has gained traction for its ability to facilitate reversible functional group exchanges without the need for external nucleophilic facilitators.[28,29] Notable examples of metathesis reactions include ester metathesis,[26,30,31] olefin metathesis,[32,33] carbamoyl metathesis,[34] silyl ether metathesis,[35,36] acetal metathesis,[37] dioxaborolane metathesis,[38] and boroxine metathesis.[39,40] Following the Lehn group report of a novel associative C=C/C=N metathesis reaction,[41,42] both the Qu group and our group independently introduced this novel metathesis chemistry into vitrimer fabrication.[43,44] This innovative approach, characterized by its high efficiency, catalyst-free operation, and resistance to moisture, presents a promising pathway for advancing CANs research.

Fusing two different crosslinked polymer networks (A-B type fusion) remains a significant challenge in thermoset engineering due to the permanent network structure, incompatibility, limited chain mobility, and variations in thermal stabilities.[8] While polymers containing dynamic covalent bonds can theoretically undergo rearrangement or reform under specific conditions (A-A type fusion, **Scheme 1a**), A-B type fusion remains challenging when the polymers exhibit differing dynamic behaviors or activation energies for bond exchange. The Otsuka group conducted an excellent study addressing this issue by using dynamic disulfide (S-S) bonds to promote bulk interface reactions between different thermosets (**Scheme 1b-1**).[45] However, despite the strong interactions provided by topological and S-S bonds, the fusion was predominantly confined to the interfaces. Similarly, Leibler *et al.* reported surface film adhesion through the transesterification of boronic esters at the interfaces of different

thermosets (**Scheme 1b-2**).[38] Nevertheless, creating a cohesive bulk material remains challenging. Thus, developing novel and efficient strategies to achieve A-B type fusion of thermosets, extending beyond surface adhesion and into the bulk state, is a critical objective for advancing thermoset engineering and expanding their application potential.

In this work, we explore A–B type fusion of distinct thermosets via a facile solid-state C=C/C=N bond metathesis reaction (**Scheme 1c**). To validate the solid-state reactivity, we first conducted a small-molecule model study that directly demonstrated dynamic exchange between C=C and C=N bonds under solid-state conditions. In parallel, a model thermoset incorporating both linkages was synthesized to assess the efficiency of C=C/C=N bond metathesis within a crosslinked network. Both studies confirm that C=C and C=N bonds undergo efficient exchange in the solid-state. Building on these findings, we then investigated the fusion of individual thermosets, each containing either C=C or C=N bonds. Analysis of the swelling behavior, thermal properties, and mechanical characteristics of the fused samples reveals that the C=C/C=N exchange reactions extend beyond the interface, resulting in a cohesive, new recyclable thermoset with tunable properties throughout the bulk material. Moreover, adjusting the mixing ratio of the parent thermosets allows precise control over the thermal behavior, mechanical properties, E_a, and T_v of the fused networks. This study not only addresses the challenge of A-B type fusion in thermosets architectures but also introduces a novel approach for achieving robust, bulk-level integration of thermoset materials with tunable properties. It highlights the exceptional potential of C=C/C=N metathesis chemistry in advancing CANs and opening new possibilities for the development of advanced materials with enhanced performance and versatility.

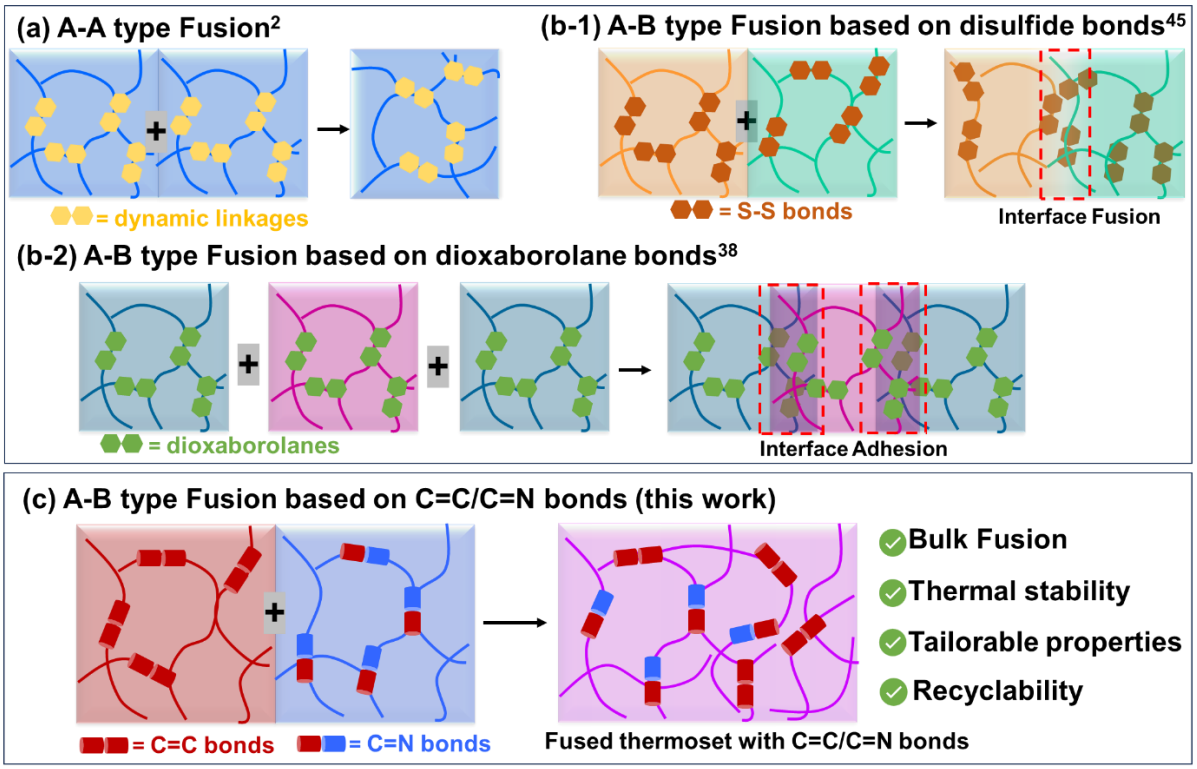

Scheme 1. State-of-the-Art approaches for (a) A-A type fusion and (b) A-B type fusion of crosslinked polymers (interface fusion); [38,45] (c) A-B type bulk fusion of two distinct crosslinked polymers using C=C/C=N exchange reactions (this work).

2. Results and Discussion

2.1 Model Studies on C=C/C=N Metathesis Reactions in solid-state

To investigate the dynamic behavior of C=C and C=N bonds under solid-state conditions, we synthesized model small molecules (Kn1, A2, Kn2, and A1), all in powder form at room temperature (**Figures 1a and 1b**). Notably, the exchange reactions between these model compounds have been confirmed in solution in our previous work,[44] providing a solid foundation for exploring their reactivity in the solid state. To ensure that reactions proceeded within the solid phase, we first determined the melting points (T_m) of the individual components using differential scanning calorimetry (DSC): Kn1 (85 °C), A2 (220 °C), Kn2 (166 °C), and A1 (45 °C) (**Figure S1**).

The Kn1/A2 binary mixture, selected as the reacting pair, exhibited a melting point of 85 °C (**Figure 1c**), establishing the upper temperature limit for preserving solid-state conditions. Solid-state reactions were subsequently conducted at 50, 55, and 60 °C, all below the melting point of the starting mixture. Equimolar amounts of Kn1 and A2 were ground together for 10 minutes to ensure uniform mixing, then subjected to hot pressing at 60 bar for 24 hours (**Figure 1b**). The resulting materials were analyzed by solid-state UV-Vis spectroscopy (**Figures 1d, and 1e**). As the temperature increased from room temperature to 60 °C, the reflectance spectra showed progressive decreases in intensity within the 300–400 nm and 420–600 nm ranges (**Figure 1d**), indicating the formation of new absorbing species. Correspondingly, Kubelka–Munk absorbance spectra revealed growing peaks at ~290 nm and ~370 nm (**Figure 1e**), consistent with the known spectral features of the products A1 and Kn2 **(Figure S2)**, confirming that the solid-state C=C and C=N bonds exchange progressed with temperature. Importantly, while one of the products, A1, has a relatively low melting point (45 °C) and may partially soften at the reaction temperatures, the system remained in the solid phase throughout. This conclusion is supported by the low conversion rate—only 7% conversion was observed even after heating at 60 °C (**Figure S3**)—indicating the absence of significant melting or phase transition. The detection of A1 under these conditions further validates that the bond exchange occurred within the solid-state.

To corroborate this conclusion, we performed solid-state ^{1}H NMR spectroscopy on the four individual compounds and the post-reaction mixtures (**Figures 1f, 1g, and S4**). The OH proton of A2 (A2-OH) was observed at ~11.78 ppm, while the OH signal of Kn2 (Kn2-OH) appeared at ~10.3 ppm. In the Kn1/A2 mixtures treated at elevated temperatures, the temperature-dependent increase in Kn2–OH signal intensity

(**highlighted in red, Figure 1g**) directly confirms product formation. This spectral evolution provides additional evidence for the temperature-driven solid-state C=C/ C=N bond exchange. Together, the solid-state UV-Vis and solid-state NMR results provide consistent and complementary evidence that C=C/C=N bond exchange reactions between Kn1 and A2 proceed under thermally activated solid-state conditions.

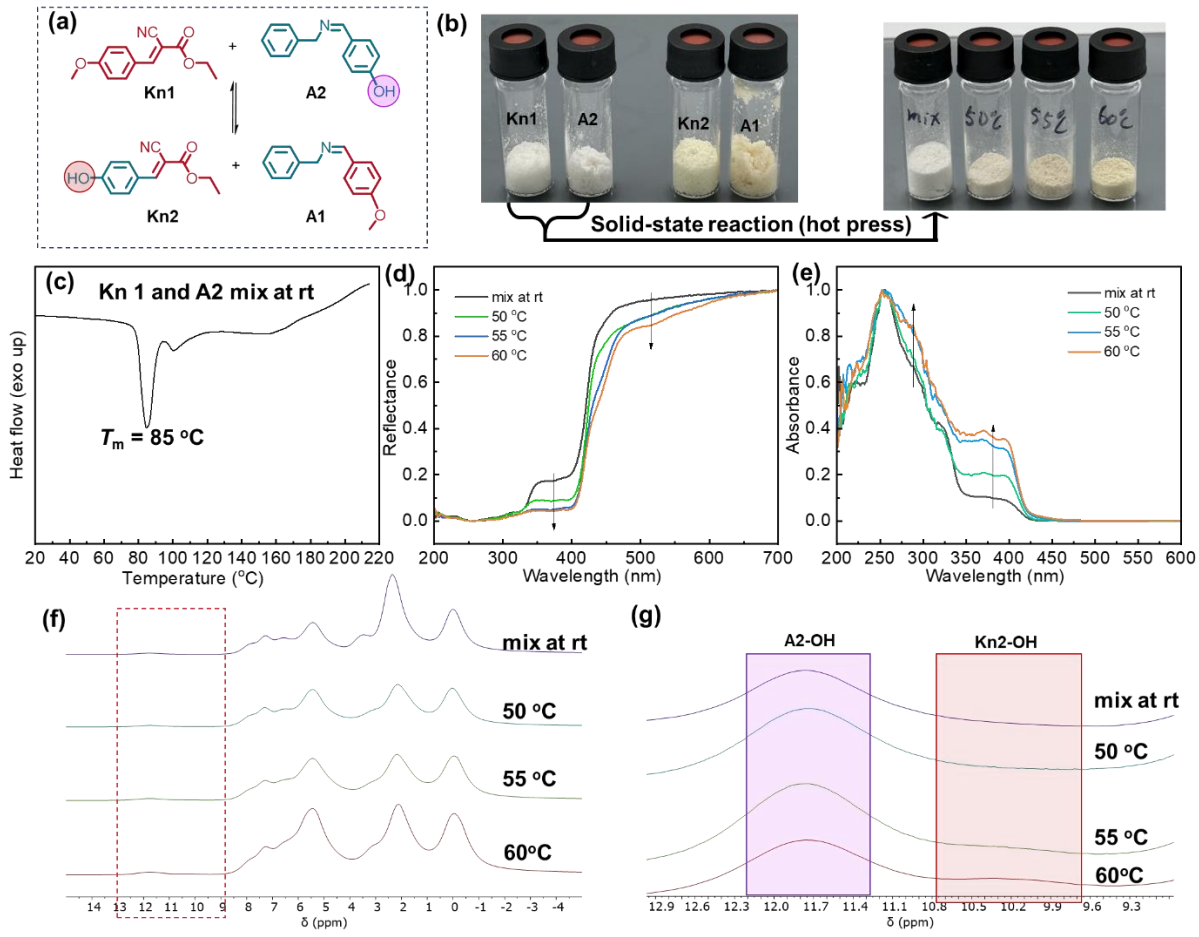

Figure 1. (a) Reaction scheme between Kn1 and A1 forming exchanged products A2 and Kn2 in the solid-state. (b) Photographs of Kn1, A2, Kn2, A1, and Kn1/A1 mixtures before reaction (rt) and after solid-state reactions at 50 °C, 55 °C, and 60 °C for 24 h. (c) DSC curve of the pre-reaction Kn1/A1 mixture. (d) Solid-state UV–Vis reflectance and (e) Kubelka–Munk absorbance spectra of the Kn1/A1 mixture before and after

reaction. (f) Solid-state ^{1}H NMR spectra and (g) zoomed-in view (13–9 ppm) highlighting OH proton regions before and after reaction at different temperatures.

To further investigate C=C/C=N bond exchange within the crosslinked polymer network, a model vitrimer (CCCN-1, **scheme S1** and **Figure S5**) was synthesized via a one-pot, catalyst-free reaction using a four-arm crosslinker (4AC; **Figure S6**). FTIR analysis confirmed successful crosslinking, as indicated by the characteristic C=C and C=N absorption bands at ~1602 and ~1641 cm^{-1}, respectively. The disappearance of the aldehyde peak from terephthalaldehyde (TPA) at ~1688 cm^{-1} further supports a high degree of monomer conversion and completion of the network formation (**Figure S7**). CCCN-1 exhibited high solvent resistance (**Figure S8, Table S1**) and excellent thermal stability ($T_{5\%}$ ~ 274 °C, **Figure S9**), confirming the formation of a densely crosslinked and thermally robust network. As shown in the storage modulus curve (**Figure S10a**), CCCN-1 exhibits a high modulus of 2000 MPa below glass transition temperature (T_g) and a rubbery plateau of 83 MPa above T_g, indicating a well-defined crosslinked structure. The corresponding crosslink density, calculated from the rubbery modulus, is 7549 mol m^{-3}. Given that creep resistance is closely tied to crosslink density, we evaluated CCCN-1's performance under thermal stress. As shown in **Figures S10b** and **S10c**, the thermoset fully recovered its strain after a creep test at temperatures up to 165 °C within 60 min, demonstrating excellent dimensional stability. Compared to other CANs,[35,37,46–53] CCCN-1 exhibited superior creep recovery at 165 °C (**Figure S10d, Table S2**), confirming that C=C/C=N bond exchange operates effectively in the solid-state and contributes to its vitrimer-like behavior. To further probe this dynamic response, stress relaxation tests were conducted at 200–230 °C using dynamic mechanical analysis (DMA). As shown in **Figure S10e**, the

modulus decayed exponentially with time, confirming vitrimer behavior driven by solid-state C=C/C=N exchange. Based on Arrhenius analysis, the E_a for the bond exchange was determined to be 66 kJ mol^{-1} (**Figure S10f**), consistent with reported values for similar dynamic systems.[44] Additionally, the CCCN-1 thermoset retained its structural integrity after recycling, as shown in **Figures S10g** and **S10h**.These results give us confidence that the C=C and C=N metathesis reactions can operate effectively in the solid-state within the thermoset network, providing a solid foundation for the subsequent A-B type fusion of individual thermosets, each containing either C=C or C=N bonds.

2.2 Fusion of Crosslinked Polymers

Fusion of different thermosets (A-B type fusion) has long posed a challenge in thermoset engineering, primarily due to their distinct dynamic behaviors and varying activation energies for bond exchange. Inspired by the high efficiency of the C=C/C=N metathesis reaction in the solid-state, we hypothesized that physically blending two thermosets, each containing either C=C or C=N bonds, could result in a uniform crosslinked polymer. This would occur through molecular-level reactions that fuse the two thermosets into a cohesive network (**Figure 2**).

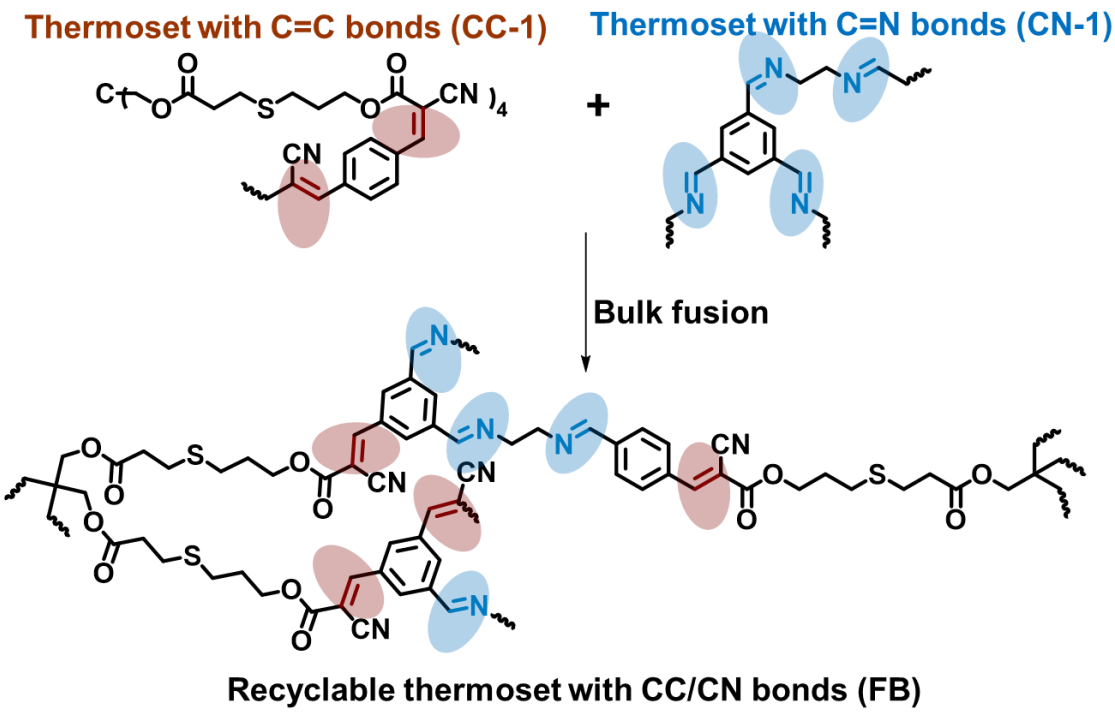

Figure 2. Schematic illustration for bulk fusion of two distinct thermosets (**CC-1** and **CN-1**), to form fused thermosets (**FB**s).

To investigate this fusion capability, two thermosets containing either C=C or C=N bonds (termed as **CC-1** and **CN-1**, respectively) were prepared and pulverized to increase their contact area for the subsequent A-B type fusion investigation (**Figures S11 and S12**). Before investigating A-B fusion, we assessed the reprocessability of **CC-1** and **CN-1** thermosets. It was found that only **CC-1** powder could be converted into a transparent film (**Figure S11g**), while **CN-1** powder could not be well reprocessed due to the low efficiency of imine bond metathesis in the absence of catalysts and active nucleophilic groups under the same hot-pressing condition (**Figure S12c**). To study the A-B fusion, powdered **CC-1** and **CN-1** were mixed in different weight ratios (*e.g.,* 2:1, 3:1, and 5:1), and the mixtures were hot-pressed at 160°C and 60 bar for 40 min to form fused thermosets, termed as ***FB*$_{2\text{-}1}$**, ***FB*$_{3\text{-}1}$**, and ***FB*$_{5\text{-}1}$**, respectively (**Figure 3,** and **Figure S13**). This solid-state fusion yields

a covalently continuous monolith, though subtle compositional gradients may persist, especially in slower-exchanging, **CN-1**–rich regions, an expected consequence of solvent-free, unstirred processing. Importantly, independent characterization confirms that the films are well fused rather than poorly integrated.

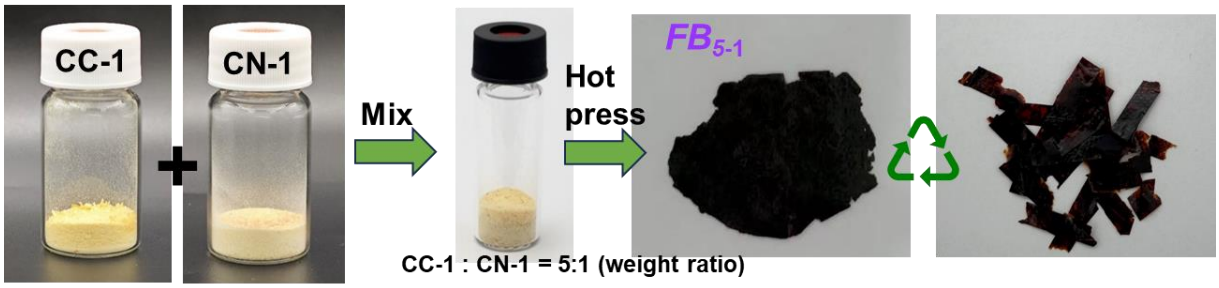

Figure 3. Photographic illustration of the fusion method used to obtain fused film (***FB*$_{5\text{-}1}$**) from **CC-1** and **CN-1** thermosets with weight ratio of 5 to 1, along with the recyclability of the resulting films.

A colour changes from light yellow to deep red/black accompanies hot pressing. This chromatic evolution likely arises from enhanced electronic coupling with local extension of conjugation, rather than formation of a fully through-bond-conjugated backbone. The substantial increase in crosslink density from the parent thermoset to the fused networks compacts the matrix and brings π-domains into closer proximity, thereby facilitating through-space π–π stacking and donor–acceptor charge-transfer (CT), potentially broadening the visible/NIR absorption (**Scheme S2**). In addition, minor thermal reactions (*e.g.,* limited elimination/oxidation) may generate local sp^2 segments/chromophores that further deepen the colour. To substantiate that the colour change reflects network formation via C=C/C=N solid-state exchange between the thermosets, FTIR and solvent-resistance assays were employed to probe the fused samples' composition and robustness. As shown in **Figure S14**, the FTIR spectra

reveal distinct peaks for both C=C (1597 cm^{-1}) and C=N (1645 cm^{-1}) bonds in all fused samples, with no new bands observed. This confirms the formation of a crosslinked network containing both C=C and C=N bonds and the absence of significant side reactions under the tested conditions (**Figure S14**). The crosslinked structure of the fused films was analyzed using swelling tests and gel fraction measurements. The samples were immersed in various solvents (DMF, DCM, THF, ACN, EtOH, and H_2O) for 48 h to reach swelling equilibrium. The results demonstrated the high stability of the fused networks in these solvents, with swelling ratios of 8% (***FB*$_{2\text{-}1}$**), 5% (***FB*$_{3\text{-}1}$**), and 7% (***FB*$_{5\text{-}1}$**) in ACN, indicating the highly crosslinked nature of the fused thermosets (**Figure S15a** and **Table S3**). Additionally, the gel fraction of the fused samples was measured in these solvents. As shown in **Figures S15b, 15c,** and **15d**, the gel content of all the fused samples remained higher than 92%. These findings confirm that the fused thermosets are robust crosslinked networks, formed through both the topological entanglement of the parent polymer chains and, more importantly, the chemical bonds generated via the C=C/C=N exchange reaction.

TGA analysis revealed that all fused samples exhibit excellent thermal stability, with $T_{5\%}$ values of 270°C, 264°C, and 281°C for ***FB*$_{2\text{-}1}$**, ***FB*$_{3\text{-}1}$**, and ***FB*$_{5\text{-}1}$**, respectively (**Figure 4a, and Table 1**). Subsequently, DSC measurements were performed to investigate compatibility of the fused thermosets (**Figure 4b**). The DSC profiles of the fused films (***FB*$_{2\text{-}1}$**, ***FB*$_{3\text{-}1}$**, and ***FB*$_{5\text{-}1}$**) showed only a single T_g (80°C, 77°C, and 55°C for ***FB*$_{2\text{-}1}$**, ***FB*$_{3\text{-}1}$**, and ***FB*$_{5\text{-}1}$**, respectively) was observed for all fused samples, regardless of the mixing ratio of the parent thermosets. This value fall between the T_g of the individual homopolymers building the thermosets (43°C for **CC-1** and 134°C for **CN-1**). These results were further corroborated by T_g measurements using DMA, which revealed a single T_g value of around 107 °C, 100°C, and 73°C for ***FB*$_{2\text{-}1}$**, ***FB*$_{3\text{-}1}$**,

and ***FB*$_{5\text{-}1}$**, respectively (**Figure 4c**). The presence of a single T_g , rather than multiple T_g values from the parent homopolymers, suggests the high miscibility of the polymer blend without phase separation.[45] Furthermore, SEM analysis confirmed the absence of any noticeable phase separation across all fused samples (**Figure S16**). These findings indicate that a homogeneous fused layer was successfully formed due to the efficient reaction between C=C bonds in **CC-1** thermoset and C=N bonds in **CN-1** thermoset.

The mechanical properties of the fused samples were evaluated using DMA. As shown in **Figure 4c**, the storage moduli of ***FB*$_{2\text{-}1}$**, ***FB*$_{3\text{-}1}$**, and ***FB*$_{5\text{-}1}$** reached maximum values of approximately 1900 MPa near 0 °C and gradually decreased with increasing temperature, reflecting the rigid and well-organized network structure of the samples in the glassy state. Above T_g, the samples displayed distinct rubbery plateaux with storage moduli of 15.84 MPa, 15.69 MPa, and 24.67 MPa, indicating a well-defined crosslinked network. The corresponding crosslink densities were calculated as 1513 mol m^{-3}, 1524 mol m^{-3}, and 2564 mol m^{-3}, respectively. The increase in crosslink density from ***FB*$_{2\text{-}1}$** to ***FB*$_{5\text{-}1}$** correlates with the rising C=C:C=N molar ratio (from 0.5:1 to 1:1), suggesting that a balanced ratio promotes more efficient C=C/C=N metathesis, leading to enhanced crosslinking. To investigate the intrinsic reactivity between C=C and C=N bonds, small-molecule model reactions between Kn1 and A2 were conducted at molar ratios of 1:1, 3:1, and 1:3. As shown in **Figure S17**, the 1:1 ratio exhibited the highest initial reaction rate, confirming that stoichiometric balance optimizes reaction kinetics. In contrast, off-stoichiometric conditions led to reduced reactivity, likely due to incomplete functional group conversion. In the ***FB*** networks, the estimated C=C:C=N molar ratios are 0.5:1, 0.7:1, and 1:1 for ***FB*$_{2\text{-}1}$**, ***FB*$_{3\text{-}1}$**, and ***FB*$_{5\text{-}1}$**, respectively (**Table 1**). Among them, ***FB*$_{5\text{-}1}$** achieves the most efficient crosslinking

and exhibits the narrowest tan δ peak, as its near-ideal stoichiometry enables a cohesive, densely interconnected network.

Tensile stress testing further corroborates these findings: as the ratio of C=C to C=N bonds increased in the fused samples, the Young's modulus rose significantly from 332.8 ± 81.9 MPa (***FB*$_{2\text{-}1}$**) to 527.9 ± 29.2 MPa (***FB*$_{5\text{-}1}$**) (**Figure 4d**). Similarly, the tensile strength improved from 16.11 ± 0.28 MPa (***FB*$_{2\text{-}1}$**) to 24.13 ± 1.18 MPa (***FB*$_{5\text{-}1}$**), while the elongation at break increased from 9.95 ± 2.71% (***FB*$_{2\text{-}1}$**) to 15.51 ± 3.84% (***FB*$_{5\text{-}1}$**) (**Figure 4d** and **Table 2**). Thus, by adjusting the ratio of C=C to C=N bonds, achieved by simply varying the mixing ratio of the parent thermosets, it is possible to precisely control both the efficiency of the metathesis exchange and the resulting mechanical properties. This tunability highlights the versatility of the fused films, enabling the design of materials with tailored mechanical properties to meet specific application requirements.

Table 1. Thermal and Mechanical Properties of fused networks and parent thermosets.

entry	**CC-1**: **CN-1** thermosets weight ratio	***C=C: C=N*** *bonds* molar ratio[a]	$T_{5\%}$ (°C)	T_g (°C)		E'_g (MPa)	E'_r (MPa)	ρ (mol m^{-3})
				DSC	DMA			
CN-1	0: 1	0: 1	305	134	/	/	/	/
***FB*$_{2\text{-}1}$**	2: 1	0.5: 1	270	80	107	1933	15.84	1513
***FB*$_{3\text{-}1}$**	3: 1	0.7: 1	264	77	100	1918	15.69	1524
***FB*$_{5\text{-}1}$**	5: 1	1: 1	281	55	73	1870	24.67	2564
CC-1	1: 0	1: 0	300	43	49	990	4.6	573

[a] The weight percentage of C=C bonds in the CC-1 thermoset is 8.2 wt%, while the weight percentage of C=N bonds in the CN-1 thermoset is 39.4 wt%.

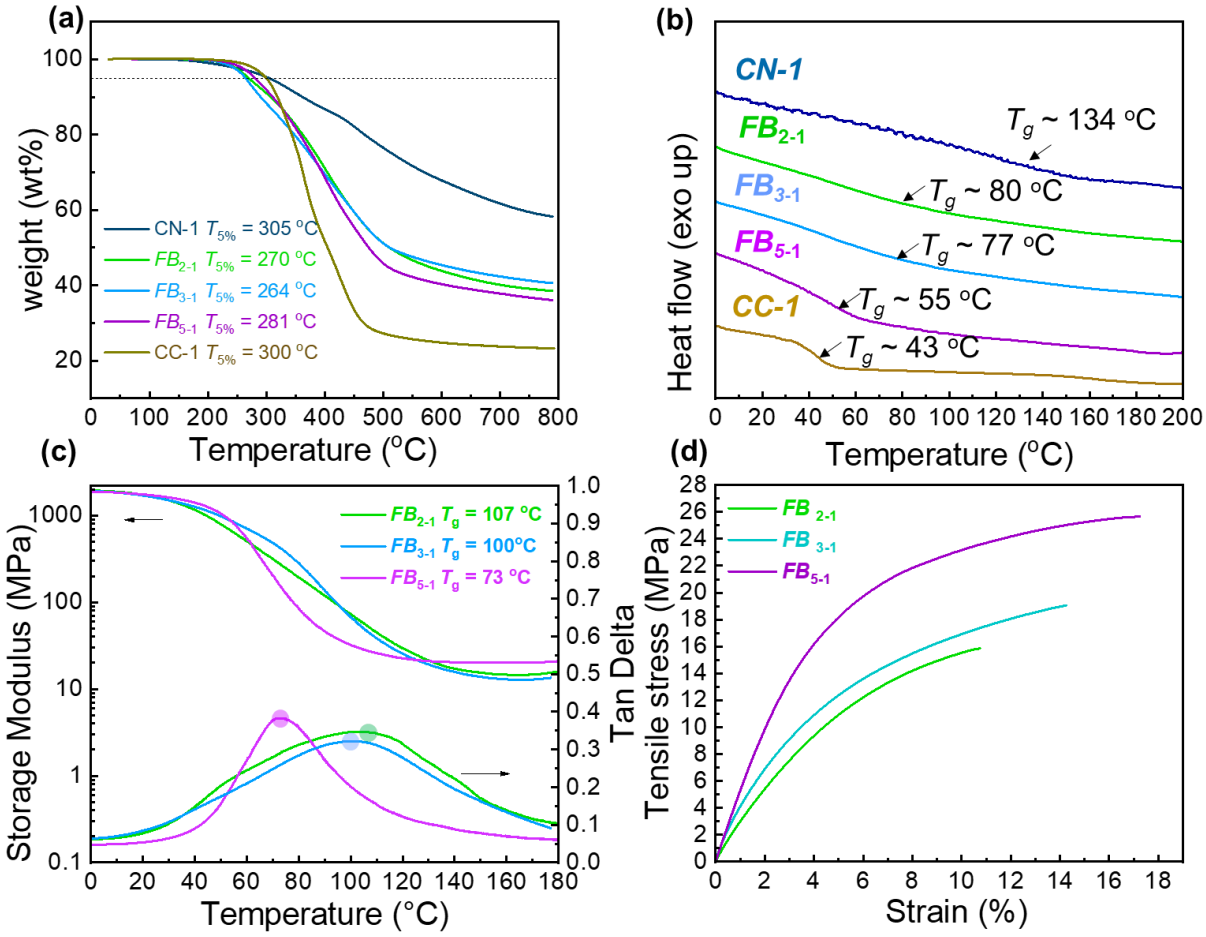

Figure 4. (a) TGA curves of the fused samples and parent thermosets (**CC-1** and **CN-1**). (b) DSC curves of the fused samples and parent thermosets (**CC-1** and **CN-1**). (c) Temperature-dependent variations in storage modulus and tan delta for fused samples. (d) Stress-strain curves illustrating the mechanical behavior of the fused samples.

Table 2. Mechanical Properties of fused networks (***FB***) and parent thermoset (**CC-1**).

Thermoset	Young's modulus (MPa)	Tensile strength (MPa)	Elongation at break (%)
***FB*$_{2-1}$**	332.8 ± 81.90	16.11 ± 0.28	9.95 ± 2.71
***FB*$_{3-1}$**	357.1 ± 67.27	18.31 ± 2.86	14.76 ± 4.44
***FB*$_{5-1}$**	527.9 ± 29.20	24.13 ± 1.18	15.51 ± 3.84
CC-1	32.21 ± 7.777	13.90 ± 1.17	177.8 ± 20.6

2.3 Dynamic nature of Fused Thermosets

The dynamic characteristics of the fused thermosets (***FB*$_{2\text{-}1}$**, ***FB*$_{3\text{-}1}$**, and ***FB*$_{5\text{-}1}$**) were investigated through stress relaxation analyses at elevated temperatures using DMA. As shown in **Figures 5a** to **5c**, the stress relaxation moduli decrease exponentially over time, indicating that the crosslinked polymers functions as vitrimers, capable of gradually relaxing stress through the dynamic C=C/C=N exchange reaction. With increasing temperature, the exchange rate accelerated, allowing the material to adapt its network (**Table S4**). Using Arrhenius' law, the E_a for the C=C/C=N exchange in the different fused thermosets was calculated to be 78 kJ mol^{-1} for ***FB*$_{2\text{-}1}$**, 75 kJ mol^{-1} for ***FB*$_{3\text{-}1}$**, and 61 kJ mol^{-1} for ***FB*$_{5\text{-}1}$** (**Figure 5d** and **table 3**). The decrease in E_a observed across the ***FB*** samples reflects the dynamic responsiveness of the network architecture. As crosslink density increases, the resulting network becomes more structurally cohesive, promoting cooperative segmental motion and more efficient stress transfer. These features facilitate bond exchange dynamics, leading to lower E_a and enhanced reprocessability and thermal adaptability.[54] Notably, ***FB*$_{5\text{-}1}$** demonstrates the most favorable dynamic behavior, consistent with its tightly interconnected structure and optimal composition. E_a is a crucial parameter, as it reflects the bond exchange reactivity and the rate at which the network viscosity changes with temperature. The ability to tune E_a by simply adjusting the parent thermosets (**CC-1** to **CN-1)** ratio provides a significant advantage: it allows for precise control over the material's stress relaxation behavior and reprocessing temperature. A lower E_a facilitates a faster exchange reaction, enabling more efficient stress relaxation and recycling at lower temperatures. This tunability enhances the versatility of the fused thermosets, making them suitable for a wide range of applications that demand varying levels of rigidity, reactivity, and recyclability.

To further evaluate the dynamic behavior of the fused networks, scratch recovery test was performed on the ***FB*** samples. In this experiment, the ***FB*** samples were scratched to introduce surface damage then subjected to thermal treatment at 180 °C. As shown in **Figures S18a to S18c**, the surface scratches nearly healed within 1 min, demonstrating rapid self-healing. Furthermore, ***FB*$_{5\text{-}1}$** showed near-complete stiffness restoration, with Young's modulus recovering to ~100%, while tensile strength and elongation at break rebounded to ~89% and ~79%, respectively, after 5 min of recovery at 180 °C (**Figure S18d,** and **18e**). This rapid surface recovery provides additional evidence of the thermally activated bond exchange behavior, reinforcing the conclusion made on the excellent reprocessability and dynamic adaptability of the fused networks at elevated temperatures.

Furthermore, the topology freezing transition temperature (T_v) of the fused thermosets can be finely tuned. T_v is a critical factor influencing the viscoelastic properties of crosslinked polymers containing dynamic covalent bonds. At T_v, the bond exchange rate becomes sufficiently rapid to transform the material from a viscoelastic solid to a viscoelastic liquid. Below T_v, crosslinked polymers maintain their structural integrity and stress relaxation capabilities due to slower bond exchange dynamics. Typically, this transition occurs when the material reaches a viscosity of 10^{12} Pa·s. The T_v of the parent thermoset **CC-1** is calculated to be 337 K, which is higher than that of all the fused samples (**Table 3**). This difference is attributed to the change in the bond exchange mechanism. In the **CC-1** thermoset, bond exchange is driven by the Knoevenagel adduct exchange, which requires a higher activation energy (E_a = 114 kJ mol^{-1}), slowing down bond dynamics and resulting in a higher T_v.[55] In contrast, the fused samples utilize C=C/C=N metathesis, facilitating bond exchange more efficiently, resulting in a lower E_a (ranging from 78 to 61 kJ mol^{-1}) and a corresponding decrease

in T_v. Furthermore, as the proportion of **CC-1** in the fused samples increases, T_v systematically decreases, from 291 K in ***FB*$_{2\text{-}1}$** to 274 K in ***FB*$_{5\text{-}1}$** (**Table 3**). This variation is due to the increased efficiency of the C=C/C=N metathesis reaction. Notably, the ***FB*$_{5\text{-}1}$** with the highest metathesis efficiency, demonstrating the lowest E_a and T_v. The tunability of both E_a and T_v enables precise control over the thermal and mechanical behavior of the fused thermosets, making them ideal for high-performance applications, including high-temperature energy storage and semiconductor packaging.

By leveraging the dynamic C=C/C=N linkages, the fused thermosets exhibit outstanding reprocessing capabilities. Following mechanical failure, the fused samples were cut into small pieces and reprocessed through hot pressing at 180°C and 50 bar for 30 min, effectively restoring the polymer network (**Figure 3a**). Tensile testing of the recycled fused thermosets revealed substantial recovery of mechanical properties. As shown in **Figure 5e**, the recycled samples exhibited high recovery rates for Young's modulus (over 100%) and tensile strength (around 80%). The reduction in elongation at break observed in the recycled samples is likely due to an increase in internal crosslinking after prolonged hot-pressing during recycling. This enhanced network structure boosts stiffness but restricts chain mobility, while potential chain scission or microstructural changes further reduce ductility. Despite this, the overall mechanical integrity of the material remains strong. Furthermore, FTIR analysis confirmed the stability of the polymer network, with no significant structural changes detected during the reprocessing process (**Figure 5f**).

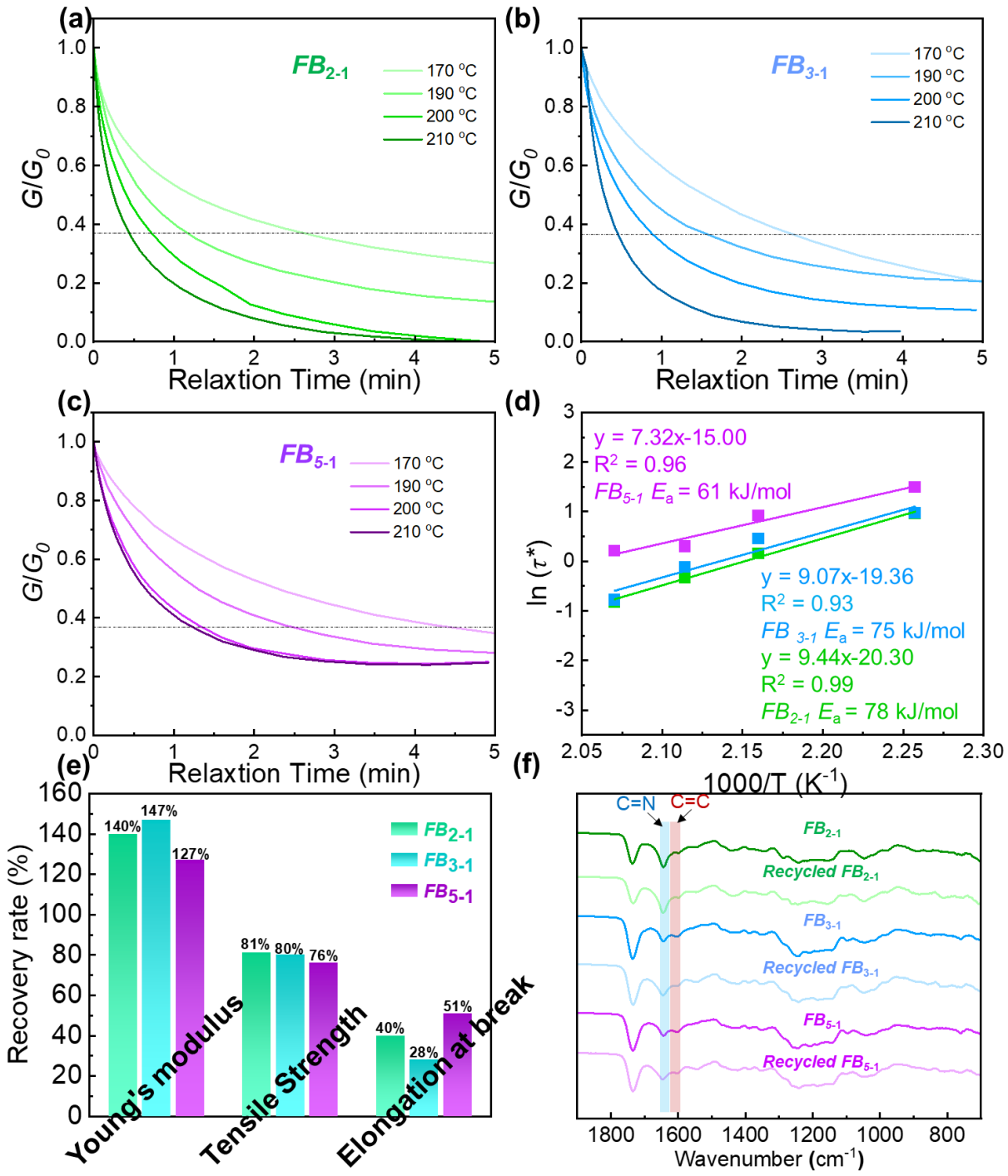

Figure 5. Stress relaxation curves of fused thermosets measured at various temperatures for (a) ***FB*$_{2\text{-}1}$**, (b) ***FB*$_{3\text{-}1}$**, and (c) ***FB*$_{5\text{-}1}$**. (d) Fitting of the relaxation times to the Arrhenius equation. (e) Recovery rates of mechanical properties after recycling for different fused thermosets. (f) Comparison of IR spectra between the original and recycled fused thermosets.

Table 3. Comparison of E_a and T_v for Different Thermosets.

Thermoset	E_a (kJ mol^{-1})	T_v (K)
***FB*$_{2\text{-}1}$**	78	291
***FB*$_{3\text{-}1}$**	75	288
***FB*$_{5\text{-}1}$**	61	274
CC-1	114	337

3.Conclusion

In conclusion, we have successfully employed solid-state C=C/C=N metathesis chemistry to achieve the fusion of distinct thermosets via dynamic covalent bond exchange. Specifically, thermosets containing either C=C or C=N bonds were effectively merged into a uniform crosslinked network featuring both functionalities. This efficient bond exchange not only enabled thermoset fusion but also resulted in advanced recyclable materials with tunable physicochemical properties. The thermal behavior, mechanical performance, E_a and T_v of the fused networks can be precisely modulated by simply varying the mixing ratio of the parent thermosets. This work represents a significant advancement in thermoset engineering, offering a versatile platform for designing high-performance materials tailored to specific application needs.

Conflicts of interest

The authors declare no competing financial interest.

ASSOCIATED CONTENT

Supporting Information

Additional experimental details, materials and characterization methods, reaction schemes, characterization data including ^{1}H NMR spectra, UV-Vis spectra, FTIR spectra, swelling rate and gel content data, TGA and DSC thermograms, photographs of chemically recycled and reprocessed polymers and their characterization data (PDF).

Acknowledgements

This project is supported by RIE2025 Manufacturing, Trade and Connectivity (MTC) Programmatic Fund (M22K9b0049, and M25O2b0016) administrated by A*STAR. N.H. gratefully acknowledges the support of the King Abdullah University of Science and Technology (KAUST).

References

(1) Ashraf, M.; Ullah, N.; Khan, I.; Tremel, W.; Ahmad, S.; Tahir, M. N. Photoreforming of Waste Polymers for Sustainable Hydrogen Fuel and Chemicals Feedstock: Waste to Energy. *Chem. Rev.* **2023**, *123* (8), 4443–4509. https://doi.org/10.1021/acs.chemrev.2c00602.

(2) Lee, K.; Jing, Y.; Wang, Y.; Yan, N. A Unified View on Catalytic Conversion of Biomass and Waste Plastics. *Nat. Rev. Chem.* **2022**, *6* (9), 635–652. https://doi.org/10.1038/s41570-022-00411-8.

(3) Coates, G. W.; Getzler, Y. D. Y. L. Chemical Recycling to Monomer for an Ideal, Circular Polymer Economy. *Nat. Rev. Mater.* **2020**, *5* (7), 501–516. https://doi.org/10.1038/s41578-020-0190-4.

(4) Yang, Y.; Xu, Y.; Ji, Y.; Wei, Y. Functional Epoxy Vitrimers and Composites.

Prog. Mater. Sci. **2021**, *120*, 100710. https://doi.org/10.1016/j.pmatsci.2020.100710.

(5) Podgórski, M.; Fairbanks, B. D.; Kirkpatrick, B. E.; McBride, M.; Martinez, A.; Dobson, A.; Bongiardina, N. J.; Bowman, C. N. Toward Stimuli-Responsive Dynamic Thermosets through Continuous Development and Improvements in Covalent Adaptable Networks (CANs). *Adv. Mater.* **2020**, *32* (20), 1–26. https://doi.org/10.1002/adma.201906876.

(6) Ma, S.; Webster, D. C. Degradable Thermosets Based on Labile Bonds or Linkages: A Review. *Prog. Polym. Sci.* **2018**, *76*, 65–110. https://doi.org/10.1016/j.progpolymsci.2017.07.008.

(7) Scheutz, G. M.; Lessard, J. J.; Sims, M. B.; Sumerlin, B. S. Adaptable Crosslinks in Polymeric Materials: Resolving the Intersection of Thermoplastics and Thermosets. *J. Am. Chem. Soc.* **2019**, *141* (41), 16181–16196. https://doi.org/10.1021/jacs.9b07922.

(8) Zheng, J.; Png, Z. M.; Ng, S. H.; Tham, G. X.; Ye, E.; Goh, S. S.; Loh, X. J.; Li, Z. Vitrimers: Current Research Trends and Their Emerging Applications. *Mater. Today* **2021**, *51*, 586–625. https://doi.org/10.1016/j.mattod.2021.07.003.

(9) Zhao, J.; Zhang, Z.; Wang, C.; Yan, X. Synergistic Dual Dynamic Bonds in Covalent Adaptable Networks. *CCS Chem.* **2023**, *6* (1), 41–56. https://doi.org/10.31635/ccschem.023.202303045.

(10) Fan, X.; Zheng, J.; Yeo, J. C. C.; Wang, S.; Li, K.; Muiruri, J. K.; Hadjichristidis, N.; Li, Z. Dynamic Covalent Bonds Enabled Carbon Fiber Reinforced Polymers Recyclability and Material Circularity. *Angew. Chemie Int. Ed.* **2024**, e202408969. https://doi.org/10.1002/anie.202408969.

(11) Denissen, W.; Winne, J. M.; Du Prez, F. E. Vitrimers: Permanent Organic

Networks with Glass-like Fluidity. *Chem. Sci.* **2016**, *7* (1), 30–38. https://doi.org/10.1039/c5sc02223a.

(12) Fortman, D. J.; Brutman, J. P.; Cramer, C. J.; Hillmyer, M. A.; Dichtel, W. R. Mechanically Activated, Catalyst-Free Polyhydroxyurethane Vitrimers. *J. Am. Chem. Soc.* **2015**, *137* (44), 14019–14022. https://doi.org/10.1021/jacs.5b08084.

(13) Yang, Y.; Terentjev, E. M.; Zhang, Y.; Chen, Q.; Zhao, Y.; Wei, Y.; Ji, Y. Reprocessable Thermoset Soft Actuators. *Angew. Chem. Int. Ed.* **2019**, *131* (48), 17635–17640. https://doi.org/10.1002/ange.201911612.

(14) Debnath, S.; Kaushal, S.; Ojha, U. Catalyst-Free Partially Bio-Based Polyester Vitrimers. *ACS Appl. Polym. Mater.* **2020**, *2* (2), 1006–1013. https://doi.org/10.1021/acsapm.0c00016.

(15) He, C.; Shi, S.; Wang, D.; Helms, B. A.; Russell, T. P. Poly(Oxime-Ester) Vitrimers with Catalyst-Free Bond Exchange. *J. Am. Chem. Soc.* **2019**, *141* (35), 13753–13757. https://doi.org/10.1021/jacs.9b06668.

(16) Delahaye, M.; Winne, J. M.; Du Prez, F. E. Internal Catalysis in Covalent Adaptable Networks: Phthalate Monoester Transesterification As a Versatile Dynamic Cross-Linking Chemistry. *J. Am. Chem. Soc.* **2019**, *141* (38), 15277–15287. https://doi.org/10.1021/jacs.9b07269.

(17) Ma, Y.; Jiang, X.; Shi, Z.; Berrocal, J. A.; Weder, C. Closed-Loop Recycling of Vinylogous Urethane Vitrimers. *Angew. Chem. Int. Ed.* **2023**, *62* (36), e202306188. https://doi.org/10.1002/anie.202306188.

(18) Guo, X.; Gao, F.; Chen, F.; Zhong, J.; Shen, L.; Lin, C.; Lin, Y. Dynamic Enamine-One Bond Based Vitrimer via Amino-Yne Click Reaction. *ACS Macro Lett.* **2021**, *10* (10), 1186–1190. https://doi.org/10.1021/acsmacrolett.1c00550.

(19) Spiesschaert, Y.; Guerre, M.; De Baere, I.; Van Paepegem, W.; Winne, J. M.; Du Prez, F. E. Dynamic Curing Agents for Amine-Hardened Epoxy Vitrimers with Short (Re)Processing Times. *Macromolecules* **2020**, *53* (7), 2485–2495. https://doi.org/10.1021/acs.macromol.9b02526.

(20) Ishibashi, J. S. A.; Kalow, J. A. Vitrimeric Silicone Elastomers Enabled by Dynamic Meldrum's Acid-Derived Cross-Links. *ACS Macro Lett.* **2018**, *7* (4), 482–486. https://doi.org/10.1021/acsmacrolett.8b00166.

(21) El-Zaatari, B. M.; Ishibashi, J. S. A.; Kalow, J. A. Cross-Linker Control of Vitrimer Flow. *Polym. Chem.* **2020**, *11* (33), 5339–5345. https://doi.org/10.1039/d0py00233j.

(22) Van Herck, N.; Maes, D.; Unal, K.; Guerre, M.; Winne, J. M.; Du Prez, F. E. Covalent Adaptable Networks with Tunable Exchange Rates Based on Reversible Thiol–Yne Cross-Linking. *Angew. Chem. Int. Ed.* **2020**, *59* (9), 3609–3617. https://doi.org/10.1002/anie.201912902.

(23) Nishimura, Y.; Chung, J.; Muradyan, H.; Guan, Z. Silyl Ether as a Robust and Thermally Stable Dynamic Covalent Motif for Malleable Polymer Design. *J. Am. Chem. Soc.* **2017**, *139* (42), 14881–14884. https://doi.org/10.1021/jacs.7b08826.

(24) Zheng, J.; Solco, S. F. D.; Wong, C. J. E.; Sia, S. A.; Tan, X. Y.; Cao, J.; Yeo, J. C. C.; Yan, W.; Zhu, Q.; Yan, Q.; Wu, J.; Suwardi, A.; Li, Z. Integrating Recyclable Polymers into Thermoelectric Devices for Green Electronics. *J. Mater. Chem. A* **2022**, *10* (37), 19787–19796. https://doi.org/10.1039/d2ta00386d.

(25) Ding, Z.; Yuan, L.; Liang, G.; Gu, A. Thermally Resistant Thermadapt Shape Memory Crosslinked Polymers Based on Silyl Ether Dynamic Covalent Linkages

for Self-Folding and Self-Deployable Smart 3D Structures. *J. Mater. Chem. A* **2019**, *7* (16), 9736–9747. https://doi.org/10.1039/c9ta01147a.

(26) Yang, S.; Liu, W.; Guo, J.; Yang, Z.; Qiao, Z.; Zhang, C.; Li, J.; Xu, J.; Zhao, N. Direct and Catalyst-Free Ester Metathesis Reaction for Covalent Adaptable Networks. *J. Am. Chem. Soc.* **2023**, *145* (38), 20927–20935. https://doi.org/10.1021/jacs.3c06262.

(27) Liu, T.; Zhao, B.; Zhang, J. Recent Development of Repairable, Malleable and Recyclable Thermosetting Polymers through Dynamic Transesterification. *Polymer (Guildf).* **2020**, *194*, 122392. https://doi.org/10.1016/j.polymer.2020.122392.

(28) Albright, H.; Davis, A. J.; Gomez-Lopez, J. L.; Vonesh, H. L.; Quach, P. K.; Lambert, T. H.; Schindler, C. S. Carbonyl-Olefin Metathesis. *Chem. Rev.* **2021**, *121* (15), 9359–9406. https://doi.org/10.1021/acs.chemrev.0c01096.

(29) Johnson, J. D.; Zhukhovitskiy, A. V. Hetero-Ene Metathesis. *ACS Catal.* **2024**, *14* (1), 21–33. https://doi.org/10.1021/acscatal.3c04135.

(30) Liu, X.; Hong, M.; Falivene, L.; Cavallo, L.; Chen, E. Y. X. Closed-Loop Polymer Upcycling by Installing Property-Enhancing Comonomer Sequences and Recyclability. *Macromolecules* **2019**, *52* (12), 4570–4578. https://doi.org/10.1021/acs.macromol.9b00817.

(31) Li, X.; Wang, L.; Li, Y.; Xu, S. Reprocessable, Self-Healing, Thermadapt Shape Memory Polycaprolactone via Robust Ester-Ester Interchanges Toward Kirigami-Tailored 4D Medical Devices. *ACS Appl. Polym. Mater.* **2023**, *5* (2), 1585–1595. https://doi.org/10.1021/acsapm.2c02070.

(32) Lu, Y. X.; Guan, Z. Olefin Metathesis for Effective Polymer Healing via Dynamic Exchange of Strong Carbon-Carbon Double Bonds. *J. Am. Chem. Soc.* **2012**,

134 (34), 14226–14231. https://doi.org/10.1021/ja306287s.

(33) Sathe, D.; Zhou, J.; Chen, H.; Su, H. W.; Xie, W.; Hsu, T. G.; Schrage, B. R.; Smith, T.; Ziegler, C. J.; Wang, J. Olefin Metathesis-Based Chemically Recyclable Polymers Enabled by Fused-Ring Monomers. *Nat. Chem.* **2021**, *13* (8), 743–750. https://doi.org/10.1038/s41557-021-00748-5.

(34) Zheng, N.; Fang, Z.; Zou, W.; Zhao, Q.; Xie, T. Thermoset Shape-Memory Polyurethane with Intrinsic Plasticity Enabled by Transcarbamoylation. *Angew. Chem. Int. Ed.* **2016**, *55* (38), 11421–11425. https://doi.org/10.1002/anie.201602847.

(35) Tretbar, C. A.; Neal, J. A.; Guan, Z. Direct Silyl Ether Metathesis for Vitrimers with Exceptional Thermal Stability. *J. Am. Chem. Soc.* **2019**, *141* (42), 16595–16599. https://doi.org/10.1021/jacs.9b08876.

(36) Khedaioui, D. Z.; Tribout, C.; Bratasanu, J.; D'Agosto, F.; Boisson, C.; Montarnal, D. Deciphering Siloxane Bond Exchanges: From a Molecular Study to Vitrimerization and Recycling of Silicone Elastomers. *Angew. Chem. Int. Ed.* **2023**, *62* (12), e202300225. https://doi.org/10.1002/anie.202300225.

(37) Li, Q.; Ma, S.; Wang, S.; Liu, Y.; Taher, M. A.; Wang, B.; Huang, K.; Xu, X.; Han, Y.; Zhu, J. Green and Facile Preparation of Readily Dual-Recyclable Thermosetting Polymers with Superior Stability Based on Asymmetric Acetal. *Macromolecules* **2020**, *53* (4), 1474–1485. https://doi.org/10.1021/acs.macromol.9b02386.

(38) Röttger, M.; Domenech, T.; Van Der Weegen, R.; Breuillac, A.; Nicolaÿ, R.; Leibler, L. High-Performance Vitrimers from Commodity Thermoplastics through Dioxaborolane Metathesis. *Science (80-.).* **2017**, *356* (6333), 62–65. https://doi.org/10.1126/science.aah5281.

(39) Ogden, W. A.; Guan, Z. Recyclable, Strong, and Highly Malleable Thermosets Based on Boroxine Networks. *J. Am. Chem. Soc.* **2018**, *140* (20), 6217–6220. https://doi.org/10.1021/jacs.8b03257.

(40) Yang, Y.; Huang, L.; Wu, R.; Fan, W.; Dai, Q.; He, J.; Bai, C. Assembling of Reprocessable Polybutadiene-Based Vitrimers with High Strength and Shape Memory via Catalyst-Free Imine-Coordinated Boroxine. *ACS Appl. Mater. Interfaces* **2020**, *12* (29), 33305–33314. https://doi.org/10.1021/acsami.0c09712.

(41) Gu, R.; Flidrova, K.; Lehn, J. M. Dynamic Covalent Metathesis in the C=C/C=N Exchange between Knoevenagel Compounds and Imines. *J. Am. Chem. Soc.* **2018**, *140* (16), 5560–5568. https://doi.org/10.1021/jacs.8b01849.

(42) Kulchat, S.; Meguellati, K.; Lehn, J. M. Organocatalyzed and Uncatalyzed C=C/C=C and C=C/C=N Exchange Processes between Knoevenagel and Imine Compounds in Dynamic Covalent Chemistry. *Helv. Chim. Acta* **2014**, *97* (9), 1219–1236. https://doi.org/10.1002/hlca.201400187.

(43) Li, P.; Jiang, X.; Gu, R.; Tian, H.; Qu, D. H. Catalyst-Free Dynamic Covalent C=C/C=N Metathesis Reaction for Associative Covalent Adaptable Networks. *Angew. Chem. Int. Ed.* **2024**, e202406708. https://doi.org/10.1002/anie.202406708.

(44) Zheng, J.; Feng, H.; Zhang, X.; Zheng, J.; Ng, J. K. W.; Wang, S.; Hadjichristidis, N.; Li, Z. Advancing Recyclable Thermosets through C═C/C═N Dynamic Covalent Metathesis Chemistry. *J. Am. Chem. Soc.* **2024**, *146* (31), 21612–21622. https://doi.org/10.1021/jacs.4c05346.

(45) Tsuruoka, A.; Takahashi, A.; Aoki, D.; Otsuka, H. Fusion of Different Crosslinked Polymers Based on Dynamic Disulfide Exchange. *Angew. Chem. Int. Ed.* **2020**,

59 (11), 4294–4298. https://doi.org/10.1002/anie.201913430.

(46) Wang, S.; Ma, S.; Li, Q.; Xu, X.; Wang, B.; Huang, K.; Liu, Y.; Zhu, J. Facile Preparation of Polyimine Vitrimers with Enhanced Creep Resistance and Thermal and Mechanical Properties via Metal Coordination. *Macromolecules* **2020**, *53* (8), 2919–2931. https://doi.org/10.1021/acs.macromol.0c00036.

(47) Lessard, J. J.; Scheutz, G. M.; Sung, S. H.; Lantz, K. A.; Epps, T. H.; Sumerlin, B. S. Block Copolymer Vitrimers. *J. Am. Chem. Soc.* **2020**, *142* (1), 283–289. https://doi.org/10.1021/jacs.9b10360.

(48) Bin Rusayyis, M. A.; Torkelson, J. M. Reprocessable Covalent Adaptable Networks with Excellent Elevated-Temperature Creep Resistance: Facilitation by Dynamic, Dissociative Bis(Hindered Amino) Disulfide Bonds. *Polym. Chem.* **2021**, *12* (18), 2760–2771. https://doi.org/10.1039/d1py00187f.

(49) You, Y.; Fu, M. R.; Rong, M. Z.; Zhang, M. Q. Improving Creep Resistance While Maintaining Reversibility of Covalent Adaptive Networks via Constructing Reversibly Interlocked Polymer Networks. *Mater. Today Chem.* **2022**, *23*, 100687. https://doi.org/10.1016/j.mtchem.2021.100687.

(50) Xu, X.; Ma, S.; Wang, S.; Wu, J.; Li, Q.; Lu, N.; Liu, Y.; Yang, J.; Feng, J.; Zhu, J. Dihydrazone-Based Dynamic Covalent Epoxy Networks with High Creep Resistance, Controlled Degradability, and Intrinsic Antibacterial Properties from Bioresources. *J. Mater. Chem. A* **2020**, *8* (22), 11261–11274. https://doi.org/10.1039/d0ta01419b.

(51) Feng, H.; Wang, S.; Lim, J. Y. C.; Li, B.; Rusli, W.; Liu, F.; Hadjichristidis, N.; Li, Z.; Zhu, J. Catalyst-Free α-Acetyl Cinnamate/Acetoacetate Exchange to Enable High Creep-Resistant Vitrimers. *Angew. Chem. Int. Ed.* **2024**, *63* (20), 100687. https://doi.org/10.1002/anie.202400955.

(52) Han, J.; Dai, M.; Bai, G.; Wei, M.; Liu, J.; Wei, W.; Liu, X.; Li, X. Azine-Based Dynamic Covalent Polyurethane Elastomers with Excellent Mechanical and Creep-Resistant Properties. *Eur. Polym. J.* **2023**, *195* (May). https://doi.org/10.1016/j.eurpolymj.2023.112210.

(53) Chen, S.; Cao, J.; Zheng, J. Reprocessable Silyl Ether-Based Dynamic Covalent Poly(Dimethylsiloxane) Networks with Superb Thermal Stability and Creep Resistance. *ACS Appl. Polym. Mater.* **2024**, *6* (7), 4215–4225. https://doi.org/10.1021/acsapm.4c00291.

(54) Wu, Z.; Chu, C.; Jin, Y.; Yang, L.; Qian, B.; Wang, Y.; Wang, Y.; Wu, J.; Jia, Y.; Zhang, W.; You, Z. Dynamic Cross-Linked Topological Network Reconciles the Longstanding Contradictory Properties of Polymers. *Sci. Adv.* **2025**, *11* (12), 1–9. https://doi.org/10.1126/sciadv.adt0825.

(55) Wang, S.; Feng, H.; Lim, J. Y. C.; Li, K.; Li, B.; Mah, J. J. Q.; Xing, Z.; Zhu, J.; Loh, X. J.; Li, Z. Recyclable, Malleable, and Strong Thermosets Enabled by Knoevenagel Adducts. *J. Am. Chem. Soc.* **2024**, *146* (14), 9920–9927. https://doi.org/10.1021/jacs.4c00043.